

## Causes of sudden, short-term changes in ice-stream surface elevation

O. V. Sergienko,<sup>1</sup> D. R. MacAyeal,<sup>2</sup> and R. A. Bindschadler<sup>3</sup>

Received 22 August 2007; revised 16 October 2007; accepted 23 October 2007; published 24 November 2007.

[1] Recent satellite-borne observations of Antarctica's ice streams show sudden, spatially confined surface-elevation changes that are interpreted as caused by subglacial water movement. Using a numerical model of idealized ice-stream flow coupled to various simple treatments of subglacial bed conditions, we demonstrate that ice-stream flow dynamics significantly modulates the surface-elevation expression of processes taking place at the ice-stream bed. This modulation means that observed surface-elevation changes do not directly translate to basal-elevation changes, e.g. inflation or deflation of subglacial water pockets, of equal magnitude and shape. Thus, subglacial water volume change is not directly proportional to the area integral of surface-elevation changes. Model results show that ambiguities in interpretation of surface elevation changes can be overcome with additional measurements, such as of surface velocity change, and through development of methodology designed to understand transfer of basal change to surface change. **Citation:** Sergienko, O. V., D. R. MacAyeal, and R. A. Bindschadler (2007), Causes of sudden, short-term changes in ice-stream surface elevation, *Geophys. Res. Lett.*, 34, L22503, doi:10.1029/2007GL031775.

### 1. Introduction

[2] Recent discoveries of sudden, meter-scale changes in surface elevation over spatially compact areas of Antarctica's ice streams made possible by various satellite-borne instruments suggest the presence of previously unknown sub-ice-stream lakes capable of rapid volume changes [Gray *et al.*, 2005; Fricker *et al.*, 2007]. This suggestion motivates the present study which examines how changes in basal conditions associated with sub-ice-stream lake development and discharge may influence surface elevation and velocity of the ice stream. As demonstrated in previous work [e.g., Gudmundsson, 2003; Raymond and Gudmundsson, 2005], the transmission of basal variability to the surface is nonlinear and complex. The patterns of surface change seen in SAR interferometry or ICESat surface altimetry [Gray *et al.*, 2005; Fricker *et al.*, 2007] are thus not necessarily translatable to simple changes in sub-ice-stream lake extent and volume without consideration of how this translation is also affected by ice-stream dynamics.

[3] The well-known stress balances of ice-stream flow [Van der Veen, 1987; Whillans and Van der Veen, 1997]

prescribe how basal resistance,  $\bar{\tau}$ , and surface elevation,  $S$ , are related via the gravitational driving stress. For example, where basal resistance is reduced, faster ice flow and mass transport cause the flow to reduce ice thickness, thereby reducing driving stress toward a new balance. Accumulation of subglacial water is a well known means to alter basal resistance. Accumulation and discharge of subglacial lakes also adds another complexity: the vertical movement of the lake "roof". When considering the causes of surface-elevation changes revealed by recent observations, it is thus reasonable to expect that changing basal resistance and lake roof elevation will combine to produce superimposed effects on the ice-stream surface elevation.

[4] To aid in the interpretation of recent ice-stream surface elevation changes, we study the effects of three phenomena that may influence ice streams as a result of subglacial water movement: (1) lowering of the ice-stream base in association with lake roof deflation, and (2) decrease and (3) increase of basal resistance independently of lake-volume changes. We use a time-dependant model of ice-stream flow and mass balance to examine these three phenomena in a simple, idealized ice-stream-flow geometry.

### 2. Model Description

[5] Our analysis is based on a finite-element model (finite-element mesh used in this study is shown in Figure S1 of the auxiliary materials)<sup>1</sup> of two-dimensional, vertically integrated ice-stream flow set in an idealized, rectangular domain  $\Gamma$  in the horizontal  $x, y$  plane. The domain dimensions are 250 km along flow and 100 km across flow, and the bed of the ice stream is inclined along the long axis of the rectangular domain, with a slope of  $10^{-3}$  (Figure 1). To represent a compact region over which changes in basal conditions will be modeled, a 10-km diameter circular subdomain,  $\Gamma_c$ , is introduced at a centered location 100 km from the inflow boundary ( $x = 0$  km) and 50 km from the side boundaries ( $y = 0, 100$  km).

[6] The variables which the model determines include the two horizontal velocity components,  $u(x, y, t)$  and  $v(x, y, t)$  in the  $x$  and  $y$  directions respectively, and the ice thickness and surface elevation  $H(x, y, t)$  and  $S(x, y, t) = H(x, y, t) + B(x, y, t)$ , respectively. Following common practice [e.g., MacAyeal, 1989], the horizontal velocities are assumed to be independent of the vertical coordinate, and the stress-balance is assumed to be quasistatic, and thus independent of time,  $t$ . The ice is also assumed to be incompressible and to obey Glen's flow law, described in the present study by a strain-rate dependent effective ice viscosity. The governing

<sup>1</sup>Oak Ridge Associated Universities at NASA Goddard Space Flight Center, Greenbelt, Maryland, USA.

<sup>2</sup>Department of the Geophysical Sciences, University of Chicago, Chicago, Illinois, USA.

<sup>3</sup>NASA Goddard Space Flight Center, Greenbelt, Maryland, USA.

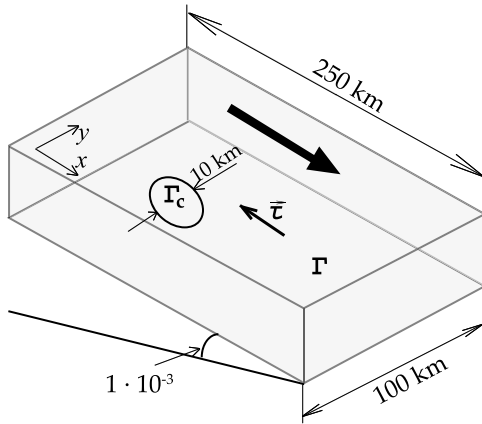


**Figure 1.** Idealized ice-stream geometry. Flow is directed along the inclination of the basal plane. Subdomain  $\Gamma_c \in \Gamma$ , represents the location of basal condition perturbations associated with subglacial lake drainage or changes in basal resistance.

stress-balance equations used to solve for  $u$  and  $v$  as a function of  $H(x, y, t)$  and  $S(x, y, t)$  are:

$$\frac{\partial}{\partial x} \left[ 2\nu H \left( 2 \frac{\partial u}{\partial x} + \frac{\partial v}{\partial y} \right) \right] + \frac{\partial}{\partial y} \left[ \nu H \left( \frac{\partial u}{\partial y} + \frac{\partial v}{\partial x} \right) \right] = \rho g H \frac{\partial S}{\partial x} - \tau_u, \quad (1)$$

$$\frac{\partial}{\partial x} \left[ \nu H \left( \frac{\partial u}{\partial y} + \frac{\partial v}{\partial x} \right) \right] + \frac{\partial}{\partial y} \left[ 2\nu H \left( \frac{\partial u}{\partial x} + 2 \frac{\partial v}{\partial y} \right) \right] = \rho g H \frac{\partial S}{\partial y} - \tau_v, \quad (2)$$

where  $\rho = 910 \text{ kg m}^{-3}$  is ice density,  $g = 9.81 \text{ m s}^{-2}$  is the acceleration due to gravity,  $\nu$  is the effective, strain-rate dependent ice viscosity representing Glen's flow law given by

$$\nu = \frac{D}{2 \left[ \left( \frac{\partial u}{\partial x} \right)^2 + \left( \frac{\partial v}{\partial y} \right)^2 + \frac{1}{4} \left( \frac{\partial u}{\partial y} + \frac{\partial v}{\partial x} \right)^2 + \frac{\partial u}{\partial x} \frac{\partial v}{\partial y} \right]^{\frac{n-1}{2n}}}, \quad (3)$$

where  $D = 1.68 \cdot 10^8 \text{ Pa s}^{1/3}$  is a vertically-averaged ice stiffness parameter,  $n = 3$  is the power-law flow exponent, and  $\tau_u$  and  $\tau_v$  are  $x$  and  $y$  components of the basal resistance, defined by

$$\begin{aligned} \tau_u &= -T \frac{u}{\sqrt{u^2 + v^2}}, \\ \tau_v &= -T \frac{v}{\sqrt{u^2 + v^2}}, \end{aligned} \quad (4)$$

and where  $T$  is a basal-resistance constant. Except within the subdomain  $\Gamma_c$ ,  $T$  is specified to be 10 kPa uniformly throughout the domain  $\Gamma$ , a value that roughly reproduces characteristic basal shear stress under fast moving ice streams in West Antarctica [Joughin *et al.*, 2004]. Equations (3) and (4) express basal resistance as plastic basal rheology. Experiments with viscous basal rheology produce results similar to ones presented here.

[7] The governing mass-balance equation is

$$\frac{\partial H}{\partial t} + \nabla \cdot (\nabla H) = \dot{A} + \dot{B}, \quad (5)$$

where  $\nabla$  is the two-dimensional divergence operator. In the present study we assume no net ablation/accumulation at the surface and melting/refreezing at the base, thus the right hand side of equation (5) is zero in all experiments.

[8] Boundary conditions on horizontal borders of  $\Gamma$  are specified to introduce a channel-like flow that is simple and representative of typical ice-stream conditions. At the two side boundaries,  $y = 0, 100 \text{ km}$  (see Figure 1),  $u$  and  $v$  are set to 0. At the upstream and downstream boundaries, no-jump conditions are specified for the vertically integrated forces in the  $x$  and  $y$  directions. The mass-balance boundary conditions are specified as follows. The ice thickness at the upstream boundary is constant  $H(x = 0, y) = 1400 \text{ m}$ , mass flux at the two side boundaries at  $y = 0, 100 \text{ km}$  is zero, and at the downstream, outflow boundary mass flux has no jump.

[9] All model experiments are transient. Their initial conditions are steady-state configurations obtained by joint iterative solution of the stress-balance and mass-balance equations with the  $\frac{\partial H}{\partial t}$  term set to zero in equation (5). The full, time-dependant model equations are run for a 10-year period to produce the results of each model experiment. A 10-year period is chosen because this time scale is consistent with the period over which observations are made by the various satellite missions.

[10] Throughout the 10-year period and at its end, ice velocity and surface elevation are compared with their initial, steady-state values. We compare ice-stream surface elevation,  $\Delta S(x, y, t > 0) = S(x, y, t) - S(x, y, 0)$ , and velocity magnitude,  $\Delta V = \sqrt{u(x, y, t)^2 + v(x, y, t)^2} - \sqrt{u(x, y, 0)^2 + v(x, y, 0)^2}$ .

### 3. Model Experiments

[11] The goal of the study is to assess ambiguities in the interpretation of ice-stream surface elevation changes in the simplest, most direct manner possible. Three experiments, denoted A, B and C, are designed for this purpose.

#### 3.1. Experiment A: Draining Lake

[12] Experiment A, the ‘‘draining lake experiment’’, aims to simulate surface elevation changes produced by gradual reduction in sub-ice-stream lake volume, represented by the gradual drop-down of the lake roof. In this experiment, the basal resistance parameter  $T$  within the circular subdomain  $\Gamma_c$  is maintained at 0 kPa to determine the steady-state initial condition, and kept at 0 kPa for the time-evolution of the ice stream over the 10-year duration of the experiment. The choice of  $T = 0$ , both in development of the initial condition and after the lake discharges, allows separation of the effects of lowering ice-stream basal elevation (lowering lake roof) from the effects of changing basal resistance. To simulate the changing volume of the lake, the basal elevation  $B$  within  $\Gamma_c$  held at the large-scale inclined value during the calculation of the steady-state initial condition, is gradually reduced during  $t > 0$  with a rate  $2 \text{ m yr}^{-1}$  during first 5 model years and then is kept constant during next 5 model years. To avoid sharp discontinuities, the reduction of

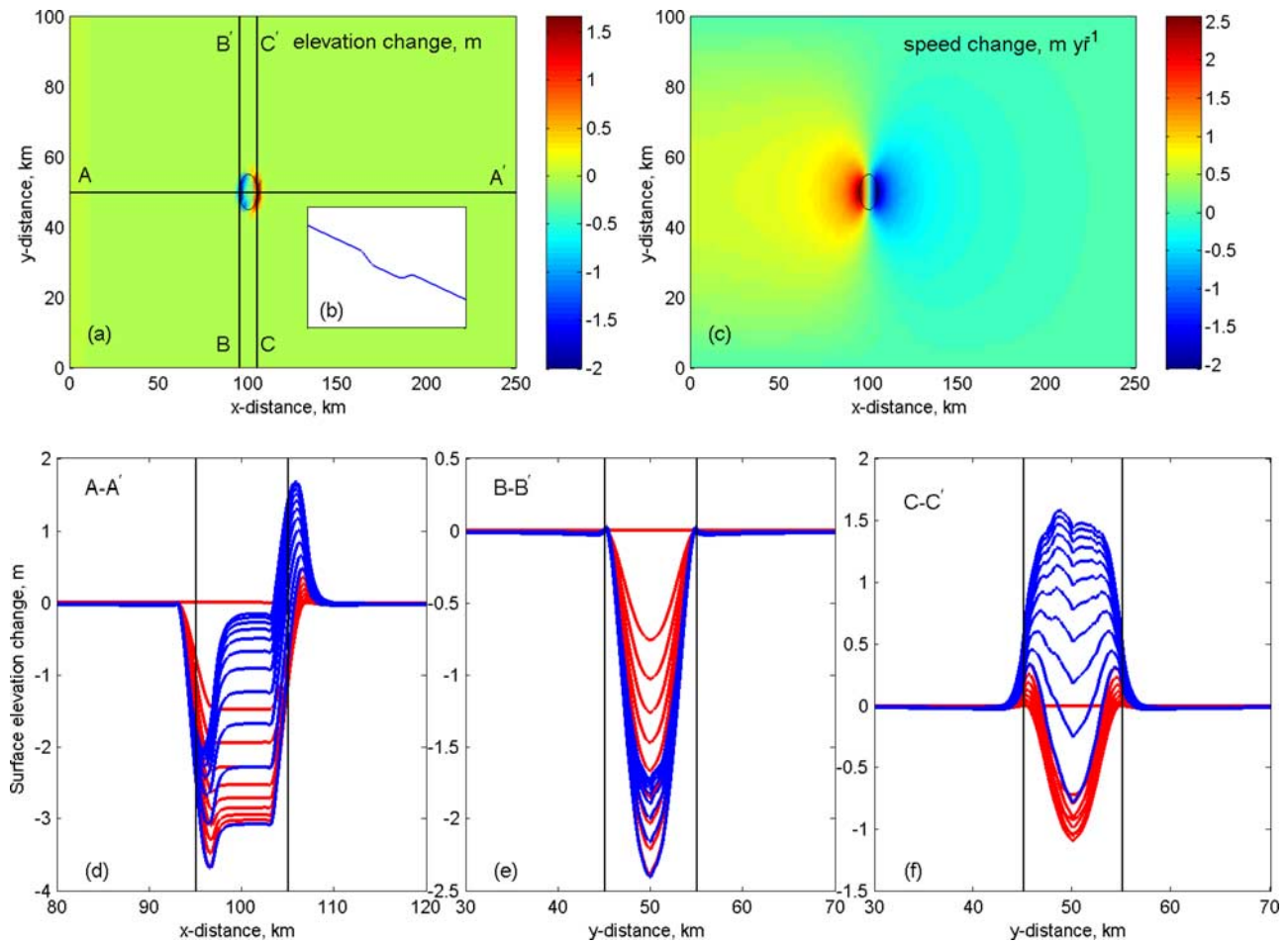


**Figure 2.** Experiment A: Ice-stream response to lowering ice base in the subdomain  $\Gamma_c$ , (a)  $\Delta S$  (m) after 10 years; (b) ice base profile at the end of the run; (c)  $\Delta V$  ( $\text{m yr}^{-1}$ ) after 2 years; (d)  $\Delta S$  (m) along the A-A' cross section; (e)  $\Delta S$  (m) along the B-B' cross section; (f)  $\Delta S$  (m) along the C-C' cross section. Cross-sections in Figures 2d–2f are shown every half of a year, red curves are the first 5 years, blue curves are the second 5 years. Vertical lines outline the extent of  $\Gamma_c$ .

$B$  is a polynomial function of  $x$  and  $y$  such that the center of  $\Gamma_c$  experiences a drop of 10 m and the edges of  $\Gamma_c$  experiences a drop that is smoothed to 0 at the edge of  $\Gamma_c$  (Figure 2b).

[13] Results of Experiment A, are presented in Figure 2. In this experiment ice speed experiences little variations. Maximum values of  $\Delta V$  are  $\sim 0.9\%$  ( $3.5 \text{ m yr}^{-1}$ ) of the initial velocity magnitude. As Figures 2d–2f show, the ice surface mimics the ice base during first years of lake drainage, but with a smaller rate of change. As the experiment proceeds, the surface lowering rate decreases with time. After two years of lake drainage, a dipole-like structure starts to develop, with zones of reduced elevation upstream and increased elevation downstream of the subdomain  $\Gamma_c$ , respectively. This pattern continues to develop over the 10-year duration of the experiment. This structure in surface elevation change develops in response to changes in slope at the upstream and downstream boundaries of  $\Gamma_c$ . At the upstream end, where the ice bed has an additional negative slope due to the initial drop of the lake's roof, ice starts to flow faster due to increased driving stress. As a result of the local increase in mass transport, ice becomes thinner and a depression is developed. An opposite situation occurs at the downstream end: the initial ice bed change has

a positive, downstream slope, that reduces local driving stress, makes the ice flow slower and induces an increase in the surface elevation to develop downstream of  $\Gamma_c$  (Figure 2c). The characteristic pattern of ice-velocity changes is a dipole with increased velocity upstream and decreased velocity downstream. After the lake discharge is complete (at  $t = 5$  years), the ice-stream surface reverses its change and starts to relax toward its initial state and eventually reaches it in  $\sim 20$  years. It is noteworthy, that the maximum drop of surface elevation is 3.8 m, while the roof of the lake drops by 10 m. This difference serves as a reminder that it is impossible to estimate of water-volume loss from area integrals of the surface elevation change without consideration of ice flow effects.

[14] Select cross-sections of  $\Delta S$  both along and across the direction of ice flow (Figures 2d–2f) are used to simulate air-borne altimetry observations which sample ice-stream surface elevation along tracks. The experimental results show that analysis of only cross-sections B-B' and C-C' does not allow an accurate assessment of the spatial pattern of  $\Delta S$ . This highlights the fact that limited sampling of  $\Delta S$  patterns in the altimetry observations can yield misleading or inaccurate estimates of sub-ice-stream lake volume changes.

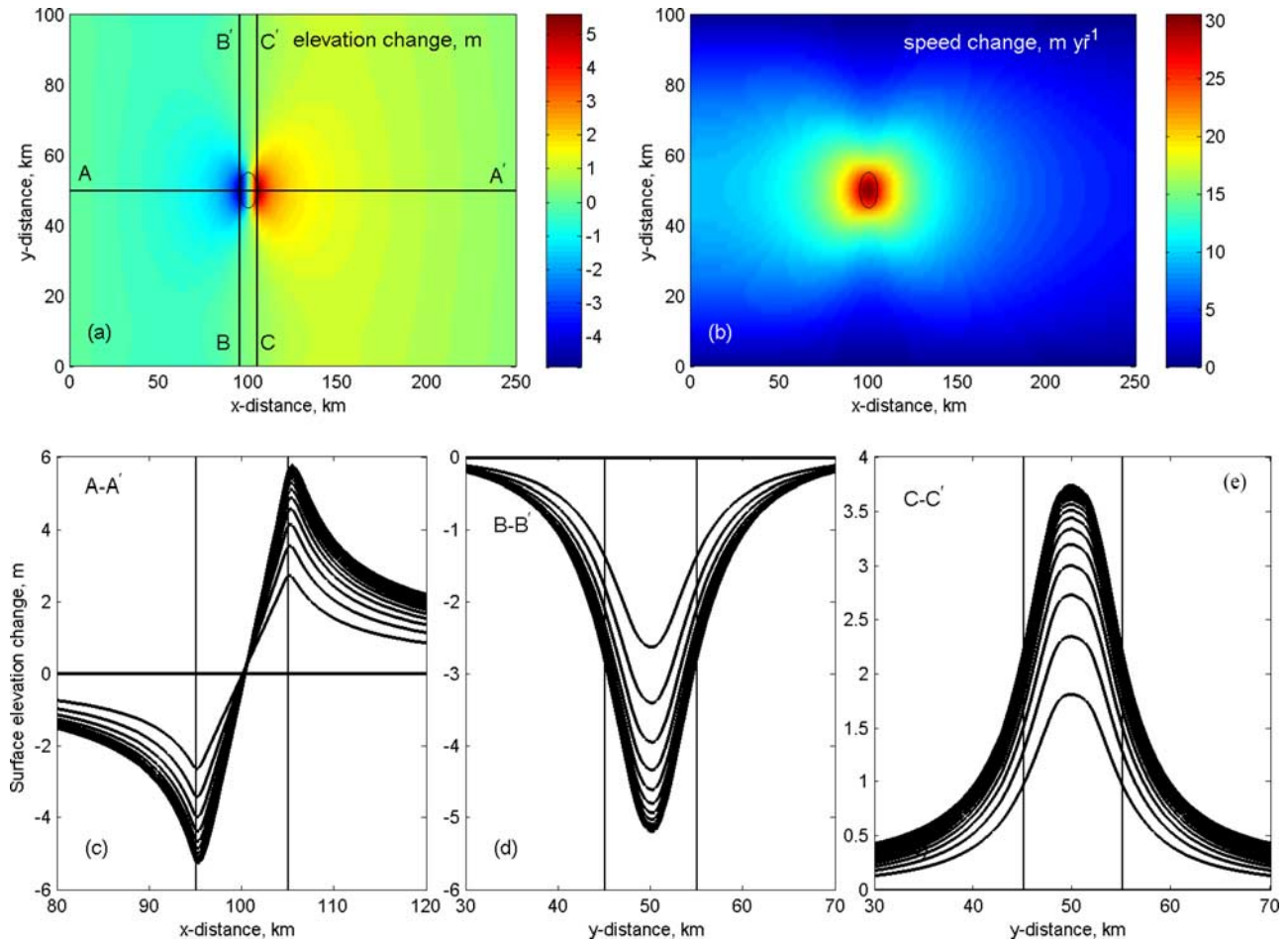


**Figure 3.** Experiment B: Ice-stream response to a sudden reduction of basal resistance in the subdomain  $\Gamma_c$ , (a)  $\Delta S$  (m) after 10 years; (b)  $\Delta V$  ( $\text{m yr}^{-1}$ ) after 2 years; (c)  $\Delta S$  along the A-A' cross section in Figure 3a; (d)  $\Delta S$  along the B-B' cross section; (e)  $\Delta S$  along the C-C' cross section. In Figures 3c–3e cross sections are shown every half year and vertical lines outline the extent of  $\Gamma_c$ .

### 3.2. Experiment B: Reduction of Basal Resistance

[15] Reduction in basal resistance is simulated by changing the basal resistance parameter  $T$  within the subdomain  $\Gamma_c$  from an initial value of 10 kPa at  $t = 0$  to 0 kPa for  $0 < t \leq 10$  years. The initial condition is the steady-state configuration of the ice stream with the uniform basal resistance parameter  $T = 10$  kPa.

[16] Results of this experiment are shown in Figure 3. A dipole with lower surface elevation upstream, and a higher surface elevation downstream of  $\Gamma_c$  develops in response to reduction of the basal resistance within  $\Gamma_c$ . The ice flowing into  $\Gamma_c$  experiences less friction, flows faster (Figure 3b) and increases mass transport, causing thinning and  $\Delta S < 0$  on the upstream side of  $\Gamma_c$ . At the downstream side of  $\Gamma_c$ , the situation is the opposite: bed resistance is stronger, the ice flows slower and mass transport is reduced. This results in ice thickening, which produces  $\Delta S > 0$ .

[17] Figures 3c–3e show surface elevation changes along various lines during the 10-year model simulation. Cross-sections taken along ice flow (Figure 3c) show development of the dipole structure described above. Cross-sections taken across ice flow show development of the surface-elevation deflation (Figure 3d) upstream, and of the surface-elevation inflation (Figure 3e) downstream of  $\Gamma_c$ . Magni-

tudes of the surface elevation changes strongly depend on a magnitude of the basal resistance reduction. To assess sensitivity of the surface elevation to the magnitude of basal resistance reduction, we have performed a set of experiments with various background basal resistances –30, 10 (present experiment), 1, 0.1 and 0.05 kPa, respectively. The corresponding maxima of surface elevation changes are 12.4, 5.6, 2.3, 0.8 and 0.02 m, respectively.

[18] Increase of the ice velocity magnitude is produced both immediately over the area with reduced basal resistance as well as over a much larger area both upstream and downstream of the subdomain  $\Gamma_c$  (Figure 3b). The maximum ice-flow increase,  $\Delta V$ , is produced over the subdomain  $\Gamma_c$ , and is more than  $50 \text{ m yr}^{-1}$  ( $\sim 15\%$ ) of the initial velocity magnitude ( $340 \text{ m yr}^{-1}$ ).

### 3.3. Experiment C: Increase of Basal Resistance

[19] Experiment C simulates a circumstance opposite to Experiment B - a sudden increase in basal traction in a limited area - to emphasize the fact that  $\Delta S$  of one sign observed in a limited region can be generated by either basal resistance change scenario. Real-world analogs for this simplified simulation can include melt-water refreezing to the ice base thereby hardening the underlying subglacial till.

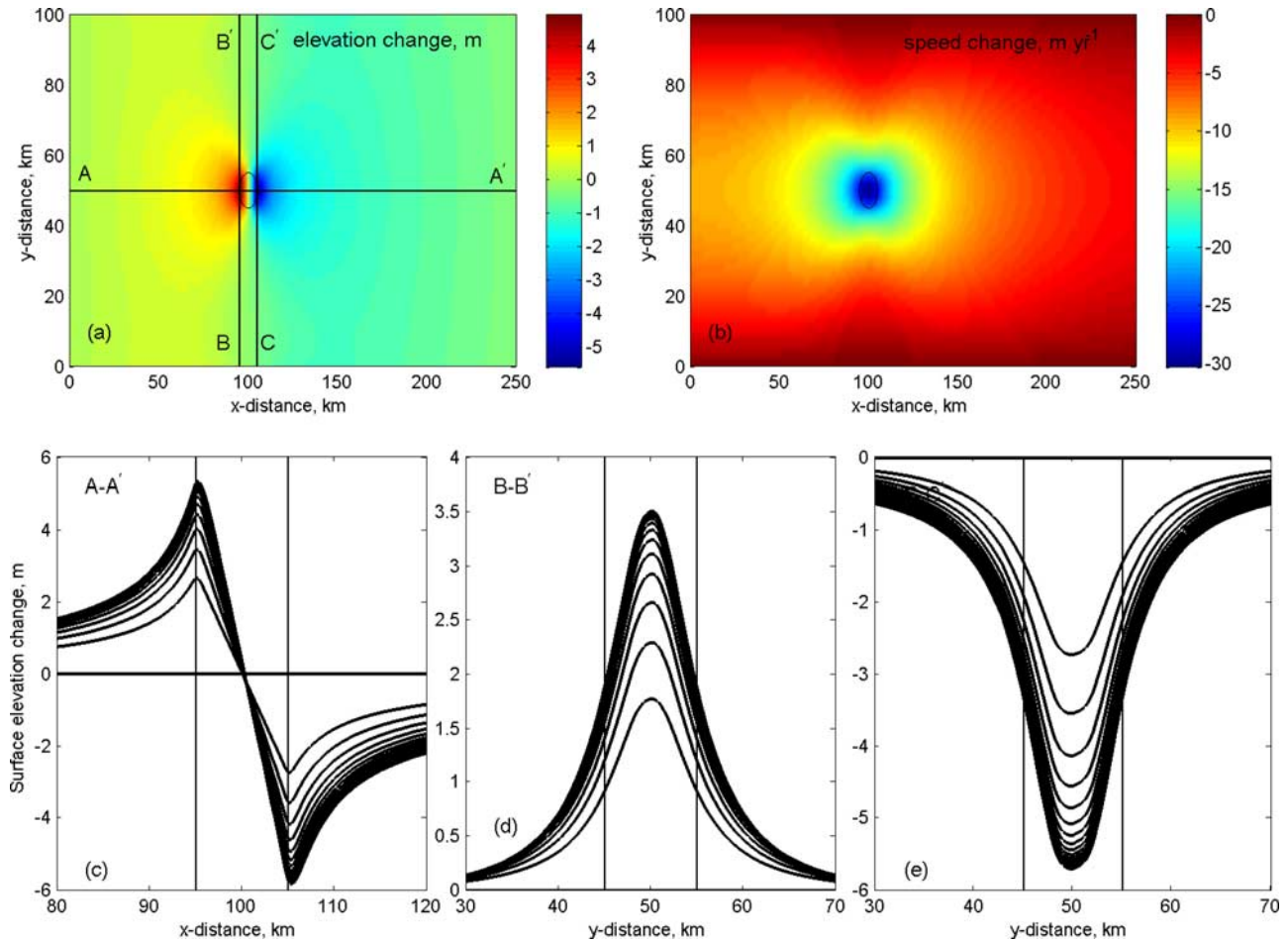


**Figure 4.** Experiment C: Ice-stream response to doubled basal resistance in the subdomain  $\Gamma_c$ . (a) surface elevation change (m) after 10 years; (b)  $\Delta V$  ( $\text{m yr}^{-1}$ ) after 2 years; (c)  $\Delta S$  along the A-A' cross section in Figure 4; (d)  $\Delta S$  along the B-B' cross section; (e)  $\Delta S$  along the C-C' cross section. In Figures 4c–4e cross sections are shown every half year and vertical lines outline the extent of  $\Gamma_c$ .

[20] In this experiment, the basal resistance parameter  $T$  in the subdomain  $\Gamma_c$  is changed from an initial value of 10 kPa at  $t = 0$  to 20 kPa for  $t > 0$ . As Figures 4a and 4c–4e show, a dipolar structure in  $\Delta S$  develops in response to such a basal resistance variation. It is similar to that of Experiment B but with opposite polarity: an uplifting zone upstream and lowering zone downstream of  $\Gamma_c$ . As in the experiment with reduced basal resistance, significant change (reduction) in ice velocity magnitude is observed over a large area (Figure 4b), with maximum change associated with the subdomain  $\Gamma_c$  (where  $\Delta V$  is  $\sim 50 \text{ m yr}^{-1}$  (15%)).

[21] Results of a “real world” lake drainage experiment - lowering of the lake roof followed by increase of its basal resistance (combination of Experiments A and C) are presented in Figure S2 of the auxiliary material. Surface elevation response to the combined forcing is complex and does not allow for making any conclusions about magnitudes of either the sub-ice-stream lake volume change or basal resistance change.

### 3.4. Conclusions

[22] Surface elevation changes observed in all experiments demonstrate the importance of ice-stream dynamics

in defining the complexity of ice stream response to changing basal conditions. Three major conclusions can be drawn from this study. First, surface elevation changes could be caused by variations in basal traction as well as by changes in sub-ice-stream lake volume. Second, ice surface response to any of such changes is complex and does not directly inform an observer about either the nature or magnitude of those changes. Third, simultaneous measurement of surface velocity would help to distinguish between surface elevation changes due to basal traction effects and those due to subglacial lake volume changes.

[23] Cross-sections of surface elevation changes obtained from the model experiments are designed to mimic the way ice-stream-surface elevation has been observed in satellite data. These cross-sections show that observed surface change [e.g., Gray *et al.*, 2005; Fricker *et al.*, 2007] is not a direct measure of the changing elevation of sub-ice-stream lake roof elevation. It is thus possible to misinterpret, for example, an observation of  $\Delta S < 0$  as signifying a reduction in lake volume, when in reality the observation may indicate a change (of either sign) of basal resistance.

[24] One possible means of differentiating between lake-drainage events and events associated with changing basal resistance is to simultaneously observe ice velocity changes.

There are clear differences in the spatial pattern of velocity change in response to these two kinds of basal forcing. In the case of a lake volume change, there is a dipole structure of velocity change over the lake. In the case of the basal resistance change, the velocity change is of one sign and is distributed over an area that is significantly larger than the area of basal change. Another distinctive feature is magnitude of velocity changes. In the case of lowering ice base it is small ( $\sim 0.9\%$  of initial velocity). In the case of the variations in basal resistance it is much larger ( $\sim 15\%$ ) and would be easily detected in repeated velocity measurements.

[25] **Acknowledgments.** We would like to thank H. A. Fricker for ICESat/GLAS data. We also thank to two anonymous reviewers whose comments and suggestions help significantly improve the manuscript. O.V.S. is supported by an appointment to the NASA Postdoctoral Program at the Goddard Space Flight Center, administered by Oak Ridge Associated Universities through a contract with NASA. Financial support for D.R.M. was provided by the National Science Foundation (NSF OPP-0229546).

## References

- Fricker, H., T. Scambos, R. Bindshadler, and L. Padman (2007), A dynamic hydraulic system beneath West Antarctic ice streams mapped from space, *Science*, *315*(5818), 1544–1548, doi:10.1126/science.1136897.
- Gray, L., I. Joughin, S. Tulaczyk, V. B. Spikes, R. Bindshadler, and K. Jezek (2005), Evidence for subglacial water transport in the West Antarctic ice sheet through three-dimensional satellite radar interferometry, *Geophys. Res. Lett.*, *32*, L03501, doi:10.1029/2004GL021387.
- Gudmundsson, G. H. (2003), Transmission of basal variability to a glacier surface, *J. Geophys. Res.*, *108*(B5), 2253, doi:10.1029/2002JB002107.
- Joughin, I., D. R. MacAyeal, and S. Tulaczyk (2004), Basal shear stress of the Ross ice streams from control method inversions, *J. Geophys. Res.*, *109*, B09405, doi:10.1029/2003JB002960.
- MacAyeal, D. R. (1989), Large-scale ice flow over a viscous basal sediment: Theory and application to ice stream-B Antarctica, *J. Geophys. Res.*, *94*(B4), 4071–4087.
- Raymond, M. J., and G. H. Gudmundsson (2005), On the relationship between surface and basal properties on glaciers, ice sheets, and ice streams, *J. Geophys. Res.*, *110*, B08411, doi:10.1029/2005JB003681.
- Van der Veen, C. (1987), Longitudinal stresses and basal sliding: A comparative study, in *Dynamics of the West Antarctic Ice Sheet*, edited by C. V. der Veen and J. Oerlemans, p. 223–248, Kluwer Acad., Norwell, Mass.
- Whillans, I., and C. Van der Veen (1997), The role of lateral drag in the dynamics of ice stream B, Antarctica, *J. Glaciol.*, *43*, 231–237.
- R. A. Bindshadler, NASA Goddard Space Flight Center, Greenbelt, MD 20771, USA.
- D. R. MacAyeal, Department of the Geophysical Sciences, University of Chicago, Chicago, IL 60637, USA.
- O. V. Sergienko, Biospheric and Hydrospheric Research Lab, Oak Ridge Associated Universities at NASA Goddard Space Flight Center, Code 614, Building 33, Room A109, Greenbelt, MD 20771, USA. (olga@neptune.gsfc.nasa.gov)